Mechanical interlocking microstructure to enhance adhesion between chemically incompatible plastics

Tim Kuipers[a], Nadine Duursma[b]

[a]employee number 909290
[b]student number 4665236

Abstract

When using incompatible materials in FDM 3D printing, the materials do not adhere well to each other. This paper aims to optimize the design of mechanically interlocking structures by maximizing its strength in order to adhere incompatible materials together as good as possible.

Table 1: Statement of Contributions

	Tim	Nadine
Introduction	✓	
Problem formulation	Straight	Diagonal
Problem investigation	Straight	Diagonal
Optimization algorithm	✓	✓
Optimization section	✓	
Results		✓
Discussion		✓
Conclusion	✓	

1. Introduction

This project is centered around the PhD research of Tim Kuipers. Therefore we have done slightly more work than necessary to obtain the right model and optimize the structure.

If one wishes to print a part consisting of two incompatible materials, an interlocking geometry is needed at the interface to make both materials mechanically adhere to each other. This can be achieved with structure that consists of parallel beams of alternating materials that interlock. Two materials were considered, a hard one (shown in green) and a soft one (in cyan), which are placed such that the interface is perpendicular to the printed layers, see Fig. 1.

The structure needs to be optimized for the highest ultimate strength of the interlocking micro-structure to maximize the force that a given area can withstand. It will be loaded in tension which is applied orthogonally to the interface. None of the components is allowed to break or yield at the highest applied force.

In addition, the structure shall be as small as possible to prevent that it affects the full part design, which is captured in both the constraints and the objective functions. The design space of both geometries is limited by the following manufacturing constraints.

- The layer height is a discrete multiple of the layer thickness $h_{\min}$.
- Any geometry height is at least $2h_{\min}$ to prevent oscillations during manufacturing.

- The total height of the micro-structure shall be less than 12 layers, therefore $h_{\max} = 12h_{\min}$.
- Any geometry length is least $2w_{\min}$ to prevent frequent retractions.
- The total length of the micro-structure shall be less than 12 layers, therefore $L_{\max} = 12w_{\min}$.
- Any geometry width is larger than the minimum manufacturable thread width $w_{\min}$, which is determined by the nozzle size.
- The total width of the micro-structure shall be less than $12w_{\min}$.

The nozzle size of the printer used is $0.4\,\mathrm{mm}$, $w_{\min}$ is estimated to be slightly lower with a value of $0.3\,\mathrm{mm}$. The layer height is set at $h_{\min} = 0.1\,\mathrm{mm}$.

Two orientations of the interlocking pattern are investigated:

Straight Even beams ('cross beams') are aligned parallel and odd beams ('fingers') are placed perpendicular to the interlocking interface, see Fig. 1.

Diagonal Even beams and odd beams (both 'fingers') are oriented at an angle with respect to the interlocking interface, see Fig. 5.

The materials that were considered are material a: Ultimaker Green Tough PLA and material b: Ultimaker Transparent PP. TPU might be considered as well in further analysis. The material properties are given in Table 2. Material a is taken as the stronger material: $\sigma_{a,\mathrm{y}} > \sigma_{b,\mathrm{y}}$. Note that 3D printed structures are anisotropic. These material properties are taken for load cases parallel to layer width since the behavior of a structure is determined mostly by the walls of a print when loaded in tension. The current model only involves σ_{yield} and $\sigma_{\mathrm{z,yield}}$. Since TPU does not yield, the ultimate strength will be used instead.

Table 2: Material properties according to Ultimaker technical data sheets.

	PLA	PP	TPU	
E	2797	302	67	MPa
E_z	2696	262	56	MPa
σ_{yield}	47	10.5	-	MPa
$\sigma_{\text{z,yield}}$	33	10.6	-	MPa
ϵ_{yield}	3.5	29	-	%
$\epsilon_{\text{z,yield}}$	2.6	22	-	%
σ_{break}	31	9.4	38	MPa
$\sigma_{\text{z,break}}$	32	10.2	6.4	MPa
ϵ_{break}	8.2	872	> 700	%
$\epsilon_{\text{z,break}}$	3.1	29	82	%
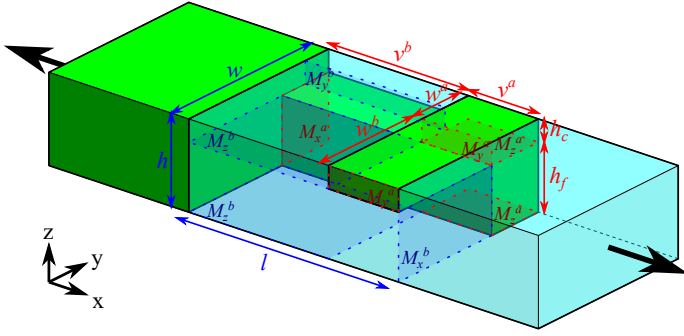
Fig. 1. One straight unit cell connecting material a (left) to material b (right). Failure can happen along the fingers (M_x), along the cross beams (M_y) or at the interface between the two (M_z) for either material.

2. Straight design

Figure 1 shows one cell of the straight design, along with the design variables and the failure modes. The aim is to optimize the effective ultimate tensile strength while keeping the perpendicular area of the structure minimal. Variables w_b, v_a, v_b, h_f and F will be optimized.

2.1. Problem Formulation

This section shows the derivation of the optimization problem.

2.1.1. Tension Failure M_x

The tensile stresses in the fingers of either material m are computed with $\frac{F}{A}$ as shown in Eq. (1).

$$\sigma_{m11} = \frac{F}{w_m h_{\text{f}}} \tag{1}$$

2.1.2. Shear Failure M_y

The shear stresses $\frac{F}{A}$ acting on $M_{\text{y},m}$ for either material m are determined by modeling the the cross beam as a cantilever beam fixed at both ends. The load is modeled as a uniformly distributed load over the whole beam. Because the beam is fixed on both sides, the shear force equals half the total force acting on the beam as shown in Eq. (2).

The parameter $d_{m,\text{y}}$ indicates the portion of the total force F which acts upon the unsupported part of material a and is proportional to w_b/w, where $w = w_a + w_b$ as given

in Eq. (3). However, in some cases the full force acts on the beam which will be discussed later. To select between these case, the parameter $u_{\text{y},m}$ can be varied between 0 and 1.

$$\sigma_{m13} = \frac{d_{m,\text{y}}F}{2v_m h_{\text{c}}} \tag{2}$$

$$d_{m,\text{y}} = \frac{w_{\neg m} + u_{\text{y},m}w_m}{w} \tag{3}$$

2.1.3. Bending Failure M_y

The highest bending stress for a doubly supported beam occurs in the middle and is given in Eq. (4).

$$\sigma_{m22} = \frac{M}{I}c = \frac{d_{m,\text{y}}Fw_{\neg m}/12}{h_{\text{c}}(v_m)^3/12}1/2v_m = \frac{d_{m,\text{y}}Fw_{\neg m}}{2\left(v_m\right)^2 h_{\text{c}}} = \sigma_{m13}\frac{w_{\neg m}}{v_m} \tag{4}$$

2.1.4. Shear Failure M_z

There is also a shear stress acting on the surface $M_{\text{z},m}$. On the one hand one might think that only a portion $d_{m,\text{z}}$ of the total force F is acting on the supported portion of the cross beam. On the other hand the total force must be enacted through this plane, because it is the only connection between the finger and the cross beam. The term $u_{\text{z},m}$ switches between a fraction of and the full force by varying it in between 0 or 1 respectively. In order to compare the stresses along the Z direction and stresses along the XY direction against the same ultimate stress value $\sigma_{m,\text{y}}$, the Z shear stress was multiplied with the ratio $\sigma_{m,\text{y}}/\sigma_{m,\text{yZ}}$. The shear stress along Z is therefore given in Eq. (5)

$$\sigma_{m12} = \frac{\sigma_{m,\text{y}}}{\sigma_{m,\text{yZ}}}\frac{d_{m,\text{z}}F}{2v_m w_m} \tag{5}$$

$$d_{m,\text{z}} = \frac{w_m + u_{\text{z},m}w_{\neg m}}{w} \tag{6}$$

2.1.5. Optimization Problem

Based on the stresses derived above, the following optimization problem was obtained.

$$f : \max \frac{F}{(w_a + w_b)(h_{\mathrm{f}} + h_{\mathrm{c}})} \tag{7}$$

subject to

$$g_1 : w_m \geq 2w_{m,\min} \qquad \text{Nozzle size} \tag{8}$$

$$g_2 : v_m \geq w_{m,\min} \qquad \text{Nozzle size} \tag{9}$$

$$g_{3f} : h_{\mathrm{f}} \geq h_{\min} \qquad \text{Layer thickness} \tag{10}$$

$$g_{3c} : h_{\mathrm{c}} \geq h_{\min} \qquad \text{Layer thickness} \tag{11}$$

$$g_4 : v_a + v_b \leq L_{\max} \qquad \text{Design constraint} \tag{12}$$

$$g_5 : \sigma_{m11} = \frac{F}{w_m h_{\mathrm{f}}} \leq \sigma_{m,\mathrm{y}} \qquad \text{Tension failure } M_{\mathrm{x},m} \tag{13}$$

$$g_{6,S} : \sigma_{m13} = \frac{F w_{\neg m}}{2 v_m h_{\mathrm{c}} w} \leq \tau_{m,\mathrm{y}} \qquad \text{Shear failure } M_{\mathrm{y},m} \tag{14}$$

$$g_{6,B} : \sigma_{m22} = \frac{F (w_{\neg m})^2}{2 (v_m)^2 h_{\mathrm{c}} w} \leq \sigma_{a,\mathrm{y}} \qquad \text{Bending failure } M_{\mathrm{y},m} \tag{15}$$

$$g_7 : \sigma_{m12} = \frac{F}{2 v_m w_m} \leq \tau_{m,\mathrm{yZ}} \qquad \text{Shear failure } M_{\mathrm{z},m} \tag{16}$$

for both materials $m \in \{a, b\}$ where $\neg a = b$ and $\neg b = a$

While the v_m variables do not appear in the objective function, they are included in the constraints are therefore also subject to the optimization. These are bounded by the active constraints.

The constraint values depend on the printer and the materials. Different nozzles and layer thickness settings require other limits on the design. Due to the manufacturing constraints, the layer thickness shall be smaller than half the smallest nozzle diameter: $h_{\min} < {}^1/2 w_{m,\min}$.

Material properties of 3D printed materials have $\tau_{m,\mathrm{yZ}} < \tau_{m,\mathrm{y}}$, since the shear strength parallel to the layers is lower due to the layer bonding.

2.1.6. Vom Mises Yield Criterion

From the von Mises yield criterion it is known that $\tau_{m,\mathrm{y}} = \sigma_{m,\mathrm{y}}/\sqrt{3}$. If $w_b/v_a > \sigma_{a,\mathrm{y}}/\tau_{a,\mathrm{y}} = \sqrt{3}$, then $\frac{d_{m,\mathrm{y}} F w_b}{2(v_a)^2 h_{\mathrm{c}} \sigma_{a,\mathrm{y}}} > \frac{d_{m,\mathrm{y}} F}{2 v_a h_{\mathrm{c}} \tau_{a,\mathrm{y}}}$. This means that the shear failure constraints Eq. (14) for material a are dominated by the bending failure constraint Eq. (15). Otherwise the latter is dominated by the former. The same holds conversely with the materials a and b swapped. Therefore, constraints Eqs. (14) and (15) can be combined.

$$\frac{d_{m,\mathrm{y}} F}{2 v_a h_{\mathrm{c}}} \max\left(\sqrt{3}, \frac{w_b}{v_a}\right) \leq \sigma_{a,\mathrm{y}}$$

$$\frac{d_{m,\mathrm{y}} F}{2 v_b h_{\mathrm{c}}} \max\left(\sqrt{3}, \frac{w_a}{v_b}\right) \leq \sigma_{b,\mathrm{y}} \tag{17}$$

The same result was obtained when using the Von Mises yield criterion directly with the shear stress σ_{13} and the bending stress σ_{22} Eq. (18).

$$(\sigma_{11} - \sigma_{22})^2 + (\sigma_{22} - \sigma_{33})^2 + (\sigma_{33} - \sigma_{11})^2$$
$$+ 6\left(\sigma_{23}^2 + \sigma_{13}^2 + \sigma_{12}^2\right) < 2\sigma_{,\mathrm{y}}2$$

$$\sigma_{a13,22} = \frac{d_{m,\mathrm{y}} F}{2 v_a h_{\mathrm{c}}} \sqrt{\left(\frac{w_b}{v_a}\right)^2 + 3} < \sigma_{a,\mathrm{y}}$$

$$\sigma_{b13,22} = \frac{d_{m,\mathrm{y}} F}{2 v_b h_{\mathrm{c}}} \sqrt{\left(\frac{w_a}{v_b}\right)^2 + 3} < \sigma_{b,\mathrm{y}} \tag{18}$$

This von Mises yield criterion Eq. (18) is equivalent to the application of the P-norm smooth approximation of the maximum function as used in the combined constraint Eq. (17), for $P = 2$.

Where $w_b/v_a \to 0$ and $w_b/v_a \to \infty$ the failure is dominated by shear and bending respectively. This shows that in the limits the von Mises yield criterion and the combined criterion coincide.

Similarly the tensile failure M_x and shear failure M_z can be combined with the von Mises criterion into $\sigma_{11,12}$. And also for Z shear failure M_z and cross beam failure M_y, including bending: $\sigma_{12,13,22}$; or without: $\sigma_{12,13}$. One might even consider a combined von Mises constraint for all stresses together: $\sigma_{11,12,13,22}$.

2.1.7. Constraint validity

A careful analysis of the geometry will show that if shearing failure mode $M_{\mathrm{x},a}$ has occurred, there is still interlocking between the two materials. If for example a part of the cross beams of b has sheared off, still a column of material a remains, which is surrounded by material b. Once one of those failure modes has occurred, still any other failure mode has to occur for the interlock to fail, except $M_{\mathrm{x},b}$. Therefore a constraint was added to the shearing failure modes that both those failure modes shall occur together. The constraint is violated only when both occur, so it is satisfied when either failure mode is prevented. The logical disjunction can be rewritten into a minimum when both constraints are transformed into negative null form:

$$\frac{d_{m,\mathrm{y}} F}{2 h_{\mathrm{c}}} \min\left(\frac{\sqrt{\left(\frac{w_b}{v_a}\right)^2 + 3}}{v_a \sigma_{a,\mathrm{y}}}, \frac{\sqrt{\left(\frac{w_a}{v_b}\right)^2 + 3}}{v_b \sigma_{b,\mathrm{y}}}\right) - 1 < 0$$

Depending on the optimization algorithm used, the min operator might need to be replaced by smooth versions. The choice between P-norm, Kreisselmeier-Steinhauser function or any of the other alternatives might be decided by properties of their derivatives. The height of the P value will determine the approximation error. The approximation error of the max function means that the approximated constraint is more strict than the underlying sub-constraints, while the smooth approximation of the min function is more lenient. This means that using a smooth approximation of this constraint could result in infeasible designs according to the analytical constraint.

Because the elongation at failure for PP is much higher than for TPLA, it is expected that in case both cross-beams break, PLA will break before PP. Therefore, the situation can be considered where the cross beam shear constraint of material a is violated and the structure will be optimized while adhering to the cross beam shear constraint of material b. See Fig. 2. In this situation the cross beam shear and bending constraints for material a do not hold. Note that after the failure mode occured, the total force cannot be uniformly distributed over the whole length w, and therefore: $u_{y,a} = \text{N/A}; u_{y,b} = 1; u_{z,a} = 1; u_{z,b} = 1$.
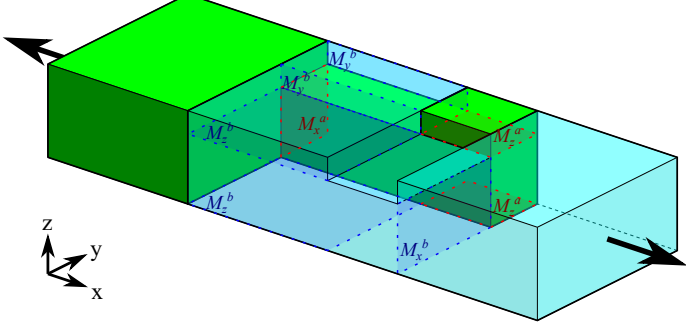
Fig. 2. The straight design if a part of the cross beam has sheared off at $M_{y,a}$.

All constraints containing the term $d_{m,y}$ can be combined into a single constraint with the following scheme:

$$\begin{matrix} h_1(\mathbf{x}) < 0 \\ \vdots \\ h_N(\mathbf{x}) < 0 \end{matrix} \rightarrow \max\left(h_1(\mathbf{x}), \ldots, h_N(\mathbf{x})\right) < 0$$

By using a smooth version of the max function like described above can overcome undifferentiability issues. However, combining all constraints into a single constraint reduces the understanding and analysis possibilities of a particular point in the design space.

2.1.8. Model Validation

When subjecting the microstructure to a load the distribution of stress is difficult to predict because of the interplay between several failure modes. The current model makes assumptions on the homogeneity of the stress distribution throughout the beams. Several modeling choices that were deferred have been mentioned: the values for $u_{y,m}$, uz, m, the exclusion of the bending constraints and using the combined von Mises criterions. In order to evaluate which analytical model is the most representative, the results of an extensive grid search were compared to FEM simulations. [1]

The grid search was performed along three dimensions: w_b, v_a and h_f, within the ranges $(0.6, 3.0)$, $(0.1L_{\max}, 0.9L_{\max})$ and $(1.8, 3.6)$ respectively. Because the design constraint is active, and also the minimum feature size is active, w_a, v_b and h_c can be derived. The output of each simulation is a force F which can be used to compute the ultimate tensile strength f of a given design.

---

[1]The FEM simulations were not performed by either of the two students that contributed to this report. Therefore the implementation details of the FEM simulation are left out.

Similarly the problem was converted such that for each design in the 3D space, the force is computed according to each mechanical constraint. For example, the minimum force according to the tensile constraint for a would be $F = \sigma_{a,y} w_a h_f$. Because the structure fails as soon as the first mechanical constraint is violated, the minimum force for all constraints is recorded and used to compute the predicted ultimate strength. Also for the comparison, $\sigma_{m,yZ}$ was set equal to $\sigma_{m,y}$ because the FEM simulations cannot anisotropic material behaviour when there is a difference in strength along the Z direction caused by the layerwise buildup of FDM 3D printing.

Table 3: Accuracy of the analytical model w.r.t. FEM results.

$u_{z,m}$	σ_{22}	$\sigma_{11,12}$	$\sigma_{12,13}$	$F/\hat{F}$	std dev
✓	-	-	-	104.2%	19.8%
✓	-	-	✓	101.7%	18.9%
✓	-	✓	✓	94.7%	19.3%
✓	-	✓	-	97.0%	20.5%
✓	✓	-	-	85.3%	31.0%
-	-	-	✓	107.6%	16.2%
-	-	-	-	107.8%	16.2%

Each point in the FEM data set was compared to the analytical model, and the average prediction ratio $F/\hat{F}$ between the simulated $\hat{F}$ and the analytically predicted F was calculated, along with the standard deviation as shown in Table 3. From these results it can be observed that including the bending stress σ_{22} does not improve the accuracy of the analytical model. Also the $\sigma_{11,12}$ von Mises criterion which combines tensile and Z shear lowers the accuracy. Using the $\sigma_{12,13}$ von Mises criterion to combine the stresses in the cross beam with the Z shear stress does improve the model.

The question whether the full force should be used to compute the Z shear stress $u_{z,m}$ is more difficult to answer; while the prediction ratio gets closer to 100%, the standard deviation increases. It makes sense that the analytical model overestimates the ultimate strength since homogenous stress distributions are assumed. Omitting $u_{z,m}$ may cause an increase in the prediction ratio, but the overall shape is closer to the FEM predictions as indicated by the lower standard deviation. Because the actual ultimate strength is less of a concern compared to obtaining the optimal design, it was chosen to only use the partial force when computing the Z shear stress.

The comparison on the final model is shown in Fig. 3. The correct value for $\sigma_{m,yZ}$ was set and the analytical model was evaluated on a more dense grid. See Fig. 4. One important observation is that four constraint surfaces can be distinguished which culminate in the same optimum, while there are only three free design variables. The four surfaces meet in a three-dimensional space, however this is not a coincidence but is presumably inherent to the particular problem at hand.

When evaluating the converted analytical model it was verified that all domain constraints are met. In this way, it was confirmed that the value for w_a and h_c can be assumed as in Section 2.1.9. Since none of the other design variables are below their lower bound, it could be concluded that these two variables had to be at their lower bound rather than any of the others.
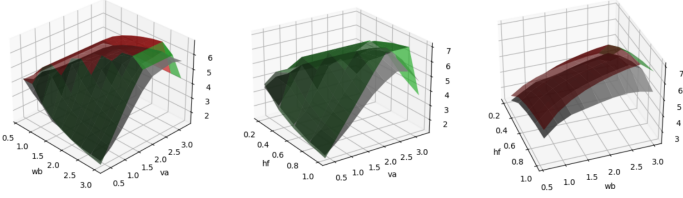
Fig. 3. Ultimate tensile strength, colored according to failure mode and FEM simulation results in gray. These are three 2D slices through the 3D space spanned by w_b, v_a and h_f, sliced at the maximum ultimate strength value.
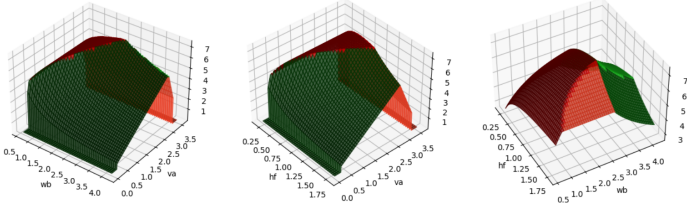
Fig. 4. Ultimate tensile strength, colored according to failure mode according to the validated model. These are three 2D slices through the 3D space spanned by w_b, v_a and h_f, sliced at the maximum ultimate strength value.

2.1.9. Problem Reformulation

Based on the findings as mentioned above, the design problem was reformulated to the negative null form. The shear constraints were combined into one. The constraints which hold for both materials were expanded. The variables set by the presumed to be active constraints were substituted.

The constraints were normalized the division of the mechanical constraints was inverted. That way the equations of those constraints are more alike and simpler to differentiate.

w_a and h_c were kept constant to disambiguate designs which have the same value for the objective function, that is: pareto optimality is introduced to disambiguate otherwise equivalent designs. If all design variables scale linearly with some factor R and F by R^2 then the objective function and all mechanical constraints Eqs. (13) to (16) remain at the same value which makes the problem underconstrained. Therefore, Eq. (8) was set to be active for material a and Eq. (11) was set to be active for h_c.

$$f : \min \frac{(2w_{a,\min} + w_b)(h_f + h_{\min})}{F}$$

$$g_1 : 1 - w_b/2w_{b,\min} \leq 0$$

$$g_{2a} : 1 - v_a/w_{a,\min} \leq 0$$

$$g_{2b} : 1 - v_b/w_{b,\min} \leq 0$$

$$g_3 : 1 - h_f/h_{\min} \leq 0$$

$$g_4 : \frac{v_a + v_b}{L_{\max}} - 1 \leq 0$$

$$g_{5a} : 1 - \frac{2w_{a,\min}h_f\sigma_{a,y}}{F} \leq 0$$

$$g_{5b} : 1 - \frac{w_b h_f \sigma_{b,y}}{F} \leq 0$$

$$g_6 : 1 - \frac{2v_a(2w_{a,\min} + w_b)\sigma_{a,y}}{F\sqrt{3\left(\frac{w_b}{h_c}\right)^2 + 3\left(\frac{\sigma_{a,y}}{\sigma_{a,yZ}}\right)^2}} \leq 0$$

$$g_7 : 1 - \frac{2v_b w_b \tau_{b,yZ}}{F} \leq 0$$

2.2. Initial Problem Investigation

This section describes the initial investigation of the optimization problem.

2.2.1. Boundedness

The optimization problem aims to maximize the strength, which scales proportionally with F and inversely with w_b and h_f. The objective function is minimized if w_b and h_f are approaching zero and if F goes to infinity. Since the minimizers $F*$, w_b* and h_f* do not lie within the set of positive and finite numbers P, the objective function is not well bounded for all of the design variables and therefore constraints are needed.

A lower bound was set on w_b and h_f with manufacturing constraints g_1 and g_3. In addition, g_5, g_6 and g_7 put an upper bound on F. Constraints g_{2a} and g_{2b} put a lower bound and constraint g_3 puts an upper bound on v_a and v_b.

2.2.2. Convexity

The objective function scales linearly with variables w_b and h_f and inversely with F. Its hessian matrix is given in Eq. (19)

$$h_f = \begin{bmatrix} 0 & 0 & 0 & \frac{1}{F} & -\frac{h_f + h_{\min}}{F^2} \\ 0 & 0 & 0 & 0 & 0 \\ 0 & 0 & 0 & 0 & 0 \\ \frac{1}{F} & 0 & 0 & 0 & -\frac{w_b + 2w_{a,\min}}{F^2} \\ -\frac{h_f + h_{\min}}{F^2} & 0 & 0 & -\frac{w_b + 2w_{a,\min}}{F^2} & \frac{2(h_f + h_{\min})(w_b + 2w_{\min})}{F^3} \end{bmatrix} \quad (19)$$

Since the principle minor of the lower left 4x4 matrix is not positive definite, the objective function is non-convex. Constraints g_1 till g_4 are linear and therefore convex. Constraints g_5 till g_7 have also an $\frac{wh}{F}$ term like f and are therefore non-convex. Because of the non-convex objective function and constraints, local minima should be accounted for in the optimization problem.

2.2.3. Monotonicity

The result of the monotonicity analysis is shown below.

$$f :F^-, w^{b+}, h_{\mathrm{f}}^+$$
$$g_1 :w^{b-}$$
$$g_{2\mathrm{a}} :v^{a-}$$
$$g_{2\mathrm{b}} :v^{b-}$$
$$g_3 :h_{\mathrm{f}}^-$$
$$g_4 :v^{a+}, v^{b+}$$
$$g_{5\mathrm{a}} :F^+, h_{\mathrm{f}}^-$$
$$g_{5\mathrm{b}} :F^+, w^{b-}, h_{\mathrm{f}}^-$$
$$g_6 :F^+, v^{a+}, w^{a+}, w^{b\pm}$$
$$g_7 :F^+, v^{b-}, w^{b-}$$

The objective function is monotonically decreasing for F, and F is monotonically increasing in constraint $g_{5\mathrm{a}}$, $g_{5\mathrm{b}}$, g_6 and g_7. Therefore one of these constraints should be active. Similarly, w_b and h_{f} are monotonically increasing in the objective function what means that constraints g_1, g_3, $g_{5\mathrm{a}}$, $g_{5\mathrm{b}}$ or g_7 can be active.

v_a and v_b not appear in the objective function are bounded by $g_{2\mathrm{a}}$, $g_{2\mathrm{b}}$ and g_4. They also appear in g_6 and g_7 which might be active as well.

2.2.4. Sensitivity Analysis

The logarithmic sensitivities were evaluated to compare the relative importance of each design variable on the objective function and the constraints. The sensitivities for the objective functions and all constraints were obtained by numerically calculating the partial derivatives with the matlab `diff` function, which were simplified afterwards. This only needs to be done once, the symbolic expressions can be reused in every iteration and because of the exact evaluation the highest accuracy is achieved.

If the numerical expression was not available, it would be recommended to use either discrete or continuum derivaties. Other methods like the finite difference method are not recommended to use because it is prone to suffer from numerical noise and it is inefficient as it cannot reuse parts from previous computations.

The logarithmic sensitivities for the objective function are given below. Since the logarithmic sensitivity of the objective with respect to the force equals -1, it means that for any given design the test force is maximized until the first failure mode will happen. The relative importance of the other design variables w_b and h_{f} depend on their magnitude, however these are expected to be smaller than 1 in magnitude.

$$\frac{\mathrm{d}_L f}{\mathrm{d}_L w_b} = \frac{w_b}{w_a + w_b}$$
$$\frac{\mathrm{d}_L f}{\mathrm{d}_L v_a} = 0$$
$$\frac{\mathrm{d}_L f}{\mathrm{d}_L v_b} = 0$$
$$\frac{\mathrm{d}_L f}{\mathrm{d}_L h_{\mathrm{f}}} = \frac{h_{\mathrm{f}}}{h_{\min} + h_{\mathrm{f}}}$$
$$\frac{\mathrm{d}_L f}{\mathrm{d}_L F} = -1$$

Similarly, the logarithmic sensitivities for the constraints were also evaluated. The non-zero logarithmic sensitivities for constraints g_1, $g_{2\mathrm{a}}$, $g_{2\mathrm{b}}$ and g_3 are shown below. These are only affected by one variable each and therefore no information on relative importance can be extracted.

$$\frac{\mathrm{d}_L g_1}{\mathrm{d}_L w_b} = \frac{w_b}{w_b - 2\, w_{b,\min}}$$
$$\frac{\mathrm{d}_L g_{2\mathrm{a}}}{\mathrm{d}_L v_a} = \frac{v_a}{v_a - w_{a,\min}}$$
$$\frac{\mathrm{d}_L g_{2\mathrm{b}}}{\mathrm{d}_L v_b} = \frac{v_b}{v_b - w_{b,\min}}$$
$$\frac{\mathrm{d}_L g_{2\mathrm{b}}}{\mathrm{d}_L h_{\mathrm{f}}} = -\frac{h_{\mathrm{f}}}{h_{\min} - h_{\mathrm{f}}}$$

Constraint g_4 is affected by two design variables v_a and v_b, their magnitudes determine their relative importance on the constraint.

$$\frac{\mathrm{d}_L g_4}{\mathrm{d}_L w_b} = 0$$
$$\frac{\mathrm{d}_L g_4}{\mathrm{d}_L v_a} = \frac{v_a}{v_a - L_{\max} + v_b}$$
$$\frac{\mathrm{d}_L g_4}{\mathrm{d}_L v_b} = \frac{v_b}{v_a - L_{\max} + v_b}$$
$$\frac{\mathrm{d}_L g_4}{\mathrm{d}_L h_{\mathrm{f}}} = 0$$
$$\frac{\mathrm{d}_L g_4}{\mathrm{d}_L F} = 0$$

In constraints $g_{5\mathrm{a}}$ and $g_{5\mathrm{b}}$, all design variables which con-

tribute to the constraint function are equally important.

$$\frac{\mathrm{d}_L g_{5\mathrm{a}}}{\mathrm{d}_L w_b} = 0$$

$$\frac{\mathrm{d}_L g_{5\mathrm{a}}}{\mathrm{d}_L v_a} = 0$$

$$\frac{\mathrm{d}_L g_{5\mathrm{a}}}{\mathrm{d}_L v_b} = 0$$

$$\frac{\mathrm{d}_L g_{5\mathrm{a}}}{\mathrm{d}_L h_{\mathrm{f}}} = -\frac{2 h_{\mathrm{f}} \sigma_{a,\mathrm{y}} w_{\min}}{2F - h_{\mathrm{f}} \sigma_{a,\mathrm{y}} w_{\min}}$$

$$\frac{\mathrm{d}_L g_{5\mathrm{a}}}{\mathrm{d}_L F} = \frac{2 h_{\mathrm{f}} \sigma_{a,\mathrm{y}} w_{\min}}{2F - h_{\mathrm{f}} \sigma_{a,\mathrm{y}} w_{\min}}$$

$$\frac{\mathrm{d}_L g_{5\mathrm{b}}}{\mathrm{d}_L w_b} = -\frac{h_{\mathrm{f}} \sigma_{b,\mathrm{y}} w_b}{F - h_{\mathrm{f}} \sigma_{b,\mathrm{y}} w_b}$$

$$\frac{\mathrm{d}_L g_{5\mathrm{b}}}{\mathrm{d}_L v_a} = 0$$

$$\frac{\mathrm{d}_L g_{5\mathrm{b}}}{\mathrm{d}_L v_b} = 0$$

$$\frac{\mathrm{d}_L g_{5\mathrm{b}}}{\mathrm{d}_L h_{\mathrm{f}}} = -\frac{h_{\mathrm{f}} \sigma_{b,\mathrm{y}} w_b}{F - h_{\mathrm{f}} \sigma_{b,\mathrm{y}} w_b}$$

$$\frac{\mathrm{d}_L g_{5\mathrm{b}}}{\mathrm{d}_L F} = \frac{h_{\mathrm{f}} \sigma_{b,\mathrm{y}} w_b}{F - h_{\mathrm{f}} \sigma_{b,\mathrm{y}} w_b}$$

The sensitivities of constraint g_6 were also obtained from the symbolic differentiation in MATLAB. However, this resulted in a long expression from which no relative influences of the design variables could be derived. Therefore only the numerical result will be presented for the derivatives of constraint g_6.

Also in constraint g_7, design variables w_b, v_b and F are all equally important.

$$\frac{\mathrm{d}_L g_7}{\mathrm{d}_L w_b} = -\frac{2\,\tau_{,\mathrm{yZ}} v_b\, w_b}{F - 2\,\tau_{,\mathrm{yZ}} v_b\, w_b}$$

$$\frac{\mathrm{d}_L g_7}{\mathrm{d}_L v_a} = 0$$

$$\frac{\mathrm{d}_L g_7}{\mathrm{d}_L v_b} = -\frac{2\,\tau_{,\mathrm{yZ}} v_b\, w_b}{F - 2\,\tau_{,\mathrm{yZ}} v_b\, w_b}$$

$$\frac{\mathrm{d}_L g_7}{\mathrm{d}_L h_{\mathrm{f}}} = 0$$

$$\frac{\mathrm{d}_L g_7}{\mathrm{d}_L F} = \frac{2\,\tau_{,\mathrm{yZ}} v_b\, w_b}{F - 2\,\tau_{,\mathrm{yZ}} v_b\, w_b}$$
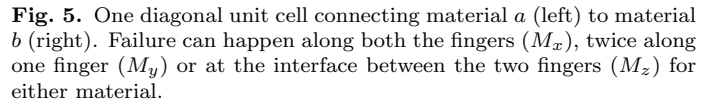
Fig. 5. One diagonal unit cell connecting material a (left) to material b (right). Failure can happen along both the fingers (M_x), twice along one finger (M_y) or at the interface between the two fingers (M_z) for either material.

3. Diagonal Design

Another option is to place the fingers under an angle as shown in Fig. 5. There are four variables: the finger width of both materials: w_a and w_b, the length L and the layer thickness h. If all four variables are scaled, then the objective function and the constrained functions scale with the same factor. Therefore, the layer thickness h will be fixed to $h = h_{\min}$ and only the variables w_a, w_b and L will be optimized.

3.1. Problem Formulation

This section shows the deriviation of the problem formulation.

3.1.1. Geometry Relations

From Fig. 5, the geometry relations Eqs. (20) to (22) can be derived, which are used for further analysis of the stresses.

$$\tan \alpha = \frac{2L}{w_a + w_b} \tag{20}$$

$$\cos \alpha = \frac{w_a + w_b}{\sqrt{(w_a + w_b)^2 + 4L^2}} \tag{21}$$

$$\sin \alpha = \frac{2L}{\sqrt{(w_a + w_b)^2 + 4L^2}} \tag{22}$$

3.1.2. Tension Failure M_x

For the tension failure, we consider the smallest cross sectional area of one finger, which is equal to $w_m h \sin \alpha$. The tensile force perpendicular to this area is equal to $\frac{F}{\sin \alpha}$, where F is the force per finger. Working out $\frac{F}{A} \leq \sigma$ resulted in Eq. (23)

$$\frac{F}{w_m h} \leq \sigma_{\max} \tag{23}$$

7

3.1.3. Shear Failure M_x

The same cross sectional area was taken as in Section 3.1.2, but now the force that is aligned with this cross section $F\cos\alpha$ is used to evaluate the shear forces. The maximum shear stress for a rectangular cross sectional area is equal to $\frac{3V}{2A}$. In this way, we derived Eq. (24)

$$\frac{3F\cos\alpha}{w_m h\sin\alpha} = \frac{3F}{w_m h\tan\alpha} \le \tau_m \tag{24}$$

We plugged in Eq. (20) what resulted in Eq. (25).

$$\frac{3F\left(w_a + w_b\right)}{4w_m h L} \le \tau_m \tag{25}$$

3.1.4. Shear Failure M_z

For a triangular cross section, the maximum shear stress is equal to $\frac{3F}{bh}$, where b and h are the base and the height of the triangle. The width and height of the rectangular area that is loaded in shear are equal to w_m and $\frac{w_m\tan\alpha}{2}$ respectively. Combining with Eq. (20) gave Eq. (26).

$$\frac{3F\left(w_a + w_b\right)}{w_m^2 L} \le \tau_m \tag{26}$$

3.1.5. Bending Failure M_x

The length of each finger, which we call l, is defined in Eq. (27)

$$l = \sqrt{\frac{\left(w_a + w_b\right)^2}{2} + L^2} \tag{27}$$

Then we can derive the moment in Eq. (28).

$$\frac{F\cos\alpha\, l}{2} = \frac{F\frac{(w_a+w_b)}{2l}l}{2} = \frac{F\left(w_a + w_b\right)}{4} \tag{28}$$

The moment of inertia I for the rectangular cross section is $\frac{h(w_m\sin\alpha)^3}{12}$. With $y = \frac{w_m\sin\alpha}{2}$, this gives a bending stress $\frac{My}{I}$ as shown in Eq. (29)

$$\frac{3F\left(w_a + w_b\right)}{2h\left(w_m\sin\alpha\right)^2} \le \sigma_m \tag{29}$$

Then we replaced $\sin\alpha$ with Eq. (22), where Eq. (30) was the final result.

$$\frac{3F\left(w_a + w_b\right)\left(\left(w_a + w_b\right)^2 + 4L^2\right)}{8hw_m^2 L^2} \le \sigma_m \tag{30}$$

3.1.6. Von Mises Stress Criterion

The tensile σ_t, bending σ_b and shear stresses τ_x acting at the section M_x were combined into the Von Mises stress criterion. The Von Mises stress is defined in Eq. (31).

$$\sqrt{\frac{\left(\sigma_t + \sigma_b\right)^2}{2} + 3\tau_x^2} \tag{31}$$

We plugged in Eqs. (23), (25) and (30), which gave Eq. (32).

$$\sqrt{\frac{1}{2}\left(\frac{F}{w_m h} + \frac{3F\left(w_a + w_b\right)\left(\left(w_a + w_b\right)^2 + 4L^2\right)}{8hw_m^2 L^2}\right)^2 + 3\left(\frac{3F\left(w_a + w_b\right)}{4w_m h L}\right)^2} \tag{32}$$

3.1.7. Optimization Problem

The goal is to maximize the strength while accounting for the failure modes in the constraints. With that, the optimization problem can be formulated as follows.

$$f: \max_{F, w_a, w_b. L} \frac{F}{2h\left(w_a + w_b\right)}$$

subject to:

$$g_1 : w_m \ge w_{m,\min}$$

$$g_2 : w_a + w_b \le w_{\max}$$

$$g_3 : L_{\min} \le L \le L_{\max}$$

$$g_4 : \frac{3F\left(w_a + w_b\right)}{w_m^2 L} \le \tau_m \text{ Shear failure } M_{z,m}$$

$$g_5 : \sqrt{\frac{1}{2}\left(\frac{F}{w_m h} + \frac{3F\left(w_a + w_b\right)\left(\left(w_a + w_b\right)^2 + 4L^2\right)}{8hw_m^2 L^2}\right)^2 + 3\left(\frac{3F\left(w_a + w_b\right)}{4w_m h L}\right)^2} \le \sigma_m$$

Von Mises criterion M_x

for both materials $m \in \{a, b\}$

3.1.8. Problem Reformulation

Constraint g_5 can be squared at both sides to get rid of the square root. Normalizing and rewriting to the negative null-form gives the following optimization problem:

$$f: \min_{F, w_a, w_b. L} \frac{2h\left(w_a + w_b\right)}{F}$$

subject to:

$$g_{1a} : 1 - \frac{w_a}{w_{a,\min}} \le 0$$

$$g_{1b} : 1 - \frac{w_b}{w_{b,\min}} \le 0$$

$$g_2 : \frac{w_a + w_b}{w_{\max}} - 1 \le 0$$

$$g_{3.1} : 1 - \frac{L}{L_{\min}} \le 0$$

$$g_{3.2} : \frac{L}{L_{\max}} - 1 \le 0$$

$$g_{4a} : \frac{3F\left(w_a + w_b\right)}{\tau_a w_a^2 L} - 1 \le 0 \text{ Shear failure } M_{z,a}$$

$$g_{4b} : \frac{3F\left(w_a + w_b\right)}{\tau_b w_b^2 L} - 1 \le 0 \text{ Shear failure } M_{z,b}$$

$$g_{5a} : \frac{\frac{1}{2}\left(\frac{F}{w_a h} + \frac{3F\left(w_a+w_b\right)\left(\left(w_a+w_b\right)^2 + 4L^2\right)}{8hw_a^2 L^2}\right)^2 + 3\left(\frac{3F\left(w_a+w_b\right)}{4w_a h L}\right)^2}{\sigma_a^2} - 1 \le 0$$

Von Mises criterion $M_{x,a}$

$$g_{5b} : \frac{\frac{1}{2}\left(\frac{F}{w_b h} + \frac{3F\left(w_a+w_b\right)\left(\left(w_a+w_b\right)^2 + 4L^2\right)}{8hw_b^2 L^2}\right)^2 + 3\left(\frac{3F\left(w_a+w_b\right)}{4w_b h L}\right)^2}{\sigma_b^2} - 1 \le 0$$

Von Mises criterion $M_{x,a}$

3.1.9. Modelling Aspects

One of the modelling aspects that should be considered is that all fingers are modelled as a cantilever beam with a

distributed load. It is assumed that every finger takes up the same load F, still one finger will fail earlier than the other because of a difference in the stress levels. Furthermore, the Von Mises stress criterion was used to predict the yielding of the material under multiple loading conditions. This does not account for the an-isotropic nature of the 3D printed material, neither for the lower infill density if larger regions are considered. It should also be noted that the adhesive bonds between the layers are weaker in shear M_z compared to the nominal shear strength. Therefore, this study should only be used as an initial investigation which needs to be tested and tuned in any case.

3.2. Initial Problem Investigation

This section discusses the initial investigation of the optimization problem.

3.2.1. Boundedness

The optimization problem aims to maximize the strength, which scales proportionally with F and inversily with the total width $w_a + w_b$ and the layer height h. f is minimized if $w_a + w_b$ and h are approaching zero and if F goes to infinity. Since the minimizers $F*$, w_a*, w_b* and $L*$ do not lie within the set of positive and finite numbers P, the objective function is not well bounded for any of the design variables and therefore constraints are needed. The layer height h was fixed and a lower bound was set on w_a and w_b with manufacturing constraint g_1. In addition, the finger length L was bounded between $L_{\min}$ and $L_{\max}$ in constraint g_3, and g_4 and g_5 put an upper bound on the force F that the fingers can withstand.

3.2.2. Convexity

The objective function f has the same format as the objective function in the straight design: $\frac{wh}{F}$ and is therefore non-convex. Constraints g_1, g_2 and g_3 are linear and therefore also convex. For constraint g_4, the Hessian matrix was evaluated, where all principle minors should be positive semi-definite for the function to be convex. A 3x3 principle minor of the full 4x4 Hessian of g_{4a} is given in Eq. (33) with partial derivatives for the design variables L, w_a and w_b.

$$H_{g,4a} = \frac{3F}{\tau_a} \begin{bmatrix} \frac{2w_a+6w_b}{(w_a)^4 L} & \frac{-2}{(w_a)^3 L} & \frac{w_a+2w_b}{(w_a)^3 L^2} \\ \frac{-2}{(w_a)^3 L} & 0 & \frac{1}{(w_a)^2 L^2} \\ \frac{w_a+2w_b}{(w_a)^3 L^2} & \frac{1}{(w_a)^2 L^2} & \frac{2(w_a+w_b)}{(w_a)^2 L^3} \end{bmatrix} \quad (33)$$

The principle minor of the upper-right 2x2 matrix of the Hessian: $\frac{-2}{(w_a)^3 L} \frac{1}{(w_a)^2 L^2} - 0$ is negative, which implies non-convexity of constraint g_4.

Inside the square root of constraint g_5, there is a bending equation contains the same dependency as g_4 and then multiplied with even more terms. This implies that g_5 is a non-convex constraint as well. The feasible domain as well as some objective functions are non-convex. Therefore local optima should be accounted for during the optimization of the problem.

3.2.3. Monotonicity

A monotonicity analysis was performed, the results are displayed below.

$$\begin{aligned} f &: F^-, w_a^+, w_b^+ \\ g_{1a} &: w_a^- \\ g_{1b} &: w_b^- \\ g_2 &: w_a^+, w_b^+ \\ g_{3.1} &: L^- \\ g_{3.2} &: L^+ \\ g_{4a} &: F^+, w_a^-, w_b^+, L^- \\ g_{4b} &: F^+, w_a^+, w_b^-, L^- \\ g_{5a} &: F^+, w_b^+, L^- \\ g_{5b} &: F^+, w_a^+, L^- \end{aligned}$$

The objective function is monotonically decreasing for F, and F is monotonically increasing in constraint g_{4a}, g_{4b}, g_{5a} and g_{5b}. This implies that one of these should be active. Similarly, w_a and w_b are monotonically increasing in the objective function. Therefore, constraints g_{1a}, g_{1b}, g_{4a} or g_{4b} should be active for w_a or w_b. L does not appear in the objective function but shall still be bounded within $L_{\min}$ and $L_{\max}$, to minimize the bending moment it is to be expected that L is close to its minimum value.

3.2.4. Sensitivity Analysis

The logarithmic sensitivities for the objective function are given below. $\dfrac{\mathrm{d}_L f}{\mathrm{d}_L w_a}$ and $\dfrac{\mathrm{d}_L f}{\mathrm{d}_L w_b}$ are always smaller than 1, therefore the variables w_a and w_b are not very influential compared to F.

$$\begin{aligned} \frac{\mathrm{d}_L f}{\mathrm{d}_L w_a} &= \frac{w_a}{w_a + w_b} \\ \frac{\mathrm{d}_L f}{\mathrm{d}_L w_b} &= \frac{w_b}{w_a + w_b} \\ \frac{\mathrm{d}_L f}{\mathrm{d}_L L} &= 0 \\ \frac{\mathrm{d}_L f}{\mathrm{d}_L F} &= -1 \end{aligned}$$

Also the logarithmic sensitivities for the constraint functions were evaluated for constraint g_1. Only variable w_a influences constraint g_{1a} and only w_b influences g_{1b}. Therefore variable w_a is a very influential parameter on g_{1a} and w_b is a very influential parameter on g_{1b}.

$$\frac{\mathrm{d}_L g_{1a}}{\mathrm{d}_L w_a} = \frac{w_a}{w_a - w_{a,\min}}$$

$$\frac{\mathrm{d}_L g_{1a}}{\mathrm{d}_L w_b} = 0$$

$$\frac{\mathrm{d}_L g_{1a}}{\mathrm{d}_L L} = 0$$

$$\frac{\mathrm{d}_L g_{1a}}{\mathrm{d}_L F} = 0$$

$$\frac{\mathrm{d}_L g_{1b}}{\mathrm{d}_L w_a} = 0$$

$$\frac{\mathrm{d}_L g_{1b}}{\mathrm{d}_L w_b} = \frac{w_b}{w_b - w_{b,\min}}$$

$$\frac{\mathrm{d}_L g_{1b}}{\mathrm{d}_L L} = 0$$

$$\frac{\mathrm{d}_L g_{1b}}{\mathrm{d}_L F} = 0$$

For constraint g_2, $w_a + w_b$ is smaller than $w_{\max}$, therefore both $\frac{\mathrm{d}_L g_2}{\mathrm{d}_L w_a}$ and $\frac{\mathrm{d}_L g_2}{\mathrm{d}_L w_b}$ are expected to be negative. The magnitude of w_a and w_b determines their relative importance.

$$\frac{\mathrm{d}_L g_2}{\mathrm{d}_L w_a} = \frac{w_a}{w_a + w_b - w_{\max}}$$

$$\frac{\mathrm{d}_L g_2}{\mathrm{d}_L w_b} = \frac{w_b}{w_a + w_b - w_{\max}}$$

$$\frac{\mathrm{d}_L g_2}{\mathrm{d}_L L} = 0$$

$$\frac{\mathrm{d}_L g_2}{\mathrm{d}_L F} = 0$$

Constraint g_3 is only influenced by L.

$$\frac{\mathrm{d}_L g_{3,1}}{\mathrm{d}_L w_a} = 0$$

$$\frac{\mathrm{d}_L g_{3,1}}{\mathrm{d}_L w_b} = 0$$

$$\frac{\mathrm{d}_L g_{3,1}}{\mathrm{d}_L L} = \frac{L}{L - L_{\min}}$$

$$\frac{\mathrm{d}_L g_{3,1}}{\mathrm{d}_L F} = 0$$

$$\frac{\mathrm{d}_L g_{3,2}}{\mathrm{d}_L w_a} = 0$$

$$\frac{\mathrm{d}_L g_{3,2}}{\mathrm{d}_L w_b} = 0$$

$$\frac{\mathrm{d}_L g_{3,2}}{\mathrm{d}_L L} = \frac{L}{L - L_{\max}}$$

$$\frac{\mathrm{d}_L g_{3,2}}{\mathrm{d}_L F} = 0$$

For constraint g_{4a}, it is known that $3F(w_a + 2w_b) > 3F(w_a + w_b) > 3Fw_b$. Therefore, design variable w_a has

the greatest influence, L and F have an equal influence and w_b has the smallest influence on constraint g_{4a}. Similarly, w_b has the greatest influence on g_{4b}, followed by an equal influence of L and F, and the smallest influence of w_a.

$$\frac{\mathrm{d}_L g_{4a}}{\mathrm{d}_L w_a} = -\frac{3\,F\,(w_a + 2\,w_b)}{-L\,\tau_{a,z}\,w_a{}^2 + 3\,F\,w_a + 3\,F\,w_b}$$

$$\frac{\mathrm{d}_L g_{4a}}{\mathrm{d}_L w_b} = \frac{3\,F\,w_b}{-L\,\tau_{a,z}\,w_a{}^2 + 3\,F\,w_a + 3\,F\,w_b}$$

$$\frac{\mathrm{d}_L g_{4a}}{\mathrm{d}_L L} = -\frac{3\,F\,(w_a + w_b)}{-L\,\tau_{a,z}\,w_a{}^2 + 3\,F\,w_a + 3\,F\,w_b}$$

$$\frac{\mathrm{d}_L g_{4a}}{\mathrm{d}_L F} = \frac{3\,F\,(w_a + w_b)}{-L\,\tau_{a,z}\,w_a{}^2 + 3\,F\,w_a + 3\,F\,w_b}$$

$$\frac{\mathrm{d}_L g_{4b}}{\mathrm{d}_L w_a} = \frac{3\,F\,w_a}{-L\,\tau_{b,z}\,w_b{}^2 + 3\,F\,w_b + 3\,F\,w_a}$$

$$\frac{\mathrm{d}_L g_{4b}}{\mathrm{d}_L w_b} = -\frac{3\,F\,(2\,w_a + w_b)}{-L\,\tau_{b,z}\,w_b{}^2 + 3\,F\,w_b + 3\,F\,w_a}$$

$$\frac{\mathrm{d}_L g_{4b}}{\mathrm{d}_L L} = -\frac{3\,F\,(w_a + w_b)}{-L\,\tau_{b,z}\,w_b{}^2 + 3\,F\,w_b + 3\,F\,w_a}$$

$$\frac{\mathrm{d}_L g_{4b}}{\mathrm{d}_L F} = \frac{3\,F\,(w_a + w_b)}{-L\,\tau_{b,z}\,w_b{}^2 + 3\,F\,w_b + 3\,F\,w_a}$$

The sensitivities of constraint g_5 were also derived, however the long expressions did not add value to the analysis. Therefore only the numerical result will be presented for the derivatives of constraint g_5.

We choose this search method because the optimum found can be used as the starting point in the optmization of the actual problem. In addition, it is easy to implement, does not suffer from getting stuck into optima and does not require the functions to be linearlized with a Taylor series approximation. It can directly be implemented to optimize the four design variables F, w_a, w_b and L. A disadvantage is that random search does not give an accurate solution if not many points are sampled, therefore the actual optimization will be done with another method.

The this resulted in a minimum objective value of 0.52 mm^2/N, obtained for the variables as indicated below.

4. Optimization Approach

The SQP algorithm was chosen to optimize problem. Given that the optimization problem is constrained, none of the unconstrained optimization methods applies. Also, given that the objective function and all of the stress values are monotonic, the surface is not expected to show high irregularies or discrete jumps. Therefore random methods like random jumping, simulated annealing would be inefficient and these are neither repeatable, which is desired when comparing two cases. The same holds for the genetic algorithm which is computationally expensive for a large population and number of iterations. Since the governing equations are available, the first and second order derivatives can be utilized to reach the optimum with less computational power. Therefore, neither Nelder-Mead Simplex nor Powell's conjugate directions were considered.

First order methods, like the conjugate gradient method can also be used, however it has a slow convergence for non

quadratic functions which appear in the design problem. Considering second order methods, SQP is the best general purpose method for differentiable constrained problems. It can handle inquality constraints with an active set strategy and it does not require a feasible starting point. Since the objective function and constraints are differentiable and SQP is expected to converge fast towards the optimum, SQP will be used to evaluated the optimization problem.

4.1. Symbolic implementation

The objective function and constraints are differentiable, however obtaining the derivative of the complex constraints is laborsome and error-prone. Therefore the Matlab builtin functionality `diff` was used to obtain the derivatives of the symbolic equations. Performing the differentiation like this is computationally intensive, but since it can be performed at the beginning of the program and the expressions can be reused in every iterations, computational time can be saved inside the main loop. The symbolic expressions are then converted to standard functions using `matlabFunction` so that they can be evaluated efficiently inside the loop.

The $\mathbf{W}$ and $\mathbf{A}$ matrices can then be constructed using $\mathbf{W} = \dfrac{\partial^2 f}{\partial \mathbf{x}^2} + \boldsymbol{\lambda}^\intercal \dfrac{\partial^2 \mathbf{h}}{\partial \mathbf{x}^2}$ and $\mathbf{A} = \dfrac{d\mathbf{h}}{d\mathbf{x}}$. Note that $\dfrac{\partial^2 \mathbf{h}}{\partial \mathbf{x}^2}$ is a precomputed 3D matrix. We can then use `quadprog` to solve $\min_{\Delta \mathbf{x}} \frac{1}{2}\Delta \mathbf{x}^\intercal \mathbf{W} \Delta \mathbf{x} + \nabla f^\intercal \Delta \mathbf{x}$ s.t. $\mathbf{A}\Delta \mathbf{x} + \mathbf{h} = \mathbf{0}$.

4.2. Active set

It was chosen to implement an active set strategy, because using slack variables or penalty and barier functions introduces inaccuracies in the final result. Here $\mathbf{h}$ is an active subset of all constraints $\mathbf{g}$, which is determined in each iteration based on the current $\mathbf{x}_k$. An approach would be to set all constraints active which are violated by the current $\mathbf{x}_k$. In order to be lenient towards numerical errors and considering that the computational accuracy is in the order of 10^{-14}, the constraint g_i was set as active when $g_i > -10^{-10}$. In this way, successive iterations along a constraint boundary will not oscillate the active set.

However, this approach can lead to issues when considering points near or beyond the global optimum. When the active set contains more constraints than design variables, the system of equations to be solved with the quadratic programming is overdetermined. In an N-dimensional space, only N hypersurfaces generally intersect in a point. It is unsure if the implemented SQP algorithm is able to deal with an active set larger than the design space.

One approach is to choose the subset of the most violated constraints. However, this will not work since the optimization will only update $\mathbf{x}_k$ if that is in favor of the objective function. No strategy was developed to deal with this problem, then the program terminates prematurely with an error message.

4.3. Lagrange multipliers

In order to compute the lambda multipliers of the outer problem, the system of linear equations: $\mathbf{A}_k = -\mathbf{W}_k \Delta \mathbf{x} - [\nabla f]_k$ is solved.

Because the active set can change each iteration, the lambda values of constraints which were unused in the previous iteration have to be revived. The full set of Lagrange multipliers is stored, out of which the active subset is picked

in each iteration. The lambda values of the previous iteration in the full set are stored, the active set is updated and then a the new set of multipliers is retrieved.

However, as the lambda values signify the relative importance of the constraints with respect to each other, the lambda values of one set cannot be reliably compared to another active set from the previous iteration. Therefore, $\boldsymbol{\lambda}$ is reset to $\mathbf{1}$ when the active set changes.

4.4. Instability prevention

In some cases the optimization occilates between two constraints, i.e. when the optimal point cycles between points on either side of two constraint surfaces. Each time the optimization is in a point $\mathbf{x}_k$ which violates some constraing g_a, it does not violate the other constraint g_b and therefore the latter is ignored. The next iteration, the same happens but then the other way around and therefore a cycle is created within the active set of constraints that is selected. Note that this is a cycle in the active set, not in $\mathbf{x}$. Therefore a strategy was invented to examine if there is a cycle when the two different active sets are repeatedly selected in the past six iterations. If there is, the new active set is forced to be the union of the two active sets in the cycle. The forced active set is alleviated after six iterations, so that new constraints can come into view of the optimization.

Another problem which occured at the beginning of the iteration loop is that the update step found by the `quadprog` function $\Delta \mathbf{x}$ becomes too large. The optimization can then quickly escalate. Therefore move limits were introduced: the magnitude of $\Delta \mathbf{x}$ was constrained to a maximum Euclidean length of 1.

4.5. Stopping criteria

The main loop of the optimization method is exited when either of several criteria is met. First, when the update step becomes too small: $|\Delta \mathbf{x}| < \mathbf{1} \cdot 10^{-10}$. This means that the algorithm converged towards a certain value. In addition the KKT conditions are checked at every iteration. `linsolve` is used to get a full set of Lagrange multipliers. It is then checked if these satisfy the optimality criterion and it is verified whether the feasibility and complementarity constraints are satisfied.

In the other cases the main loop is terminated because the optimization failed. To prevent an infinite loop, a maximum number of iterations was set to 1000. Also, in case there are more active constraints than design variables, the `quadprog` algorithm fails with an error as mentioned above. Also cycle detection was implemented, based on the values of f and $\mathbf{x}$. If the difference between the new point $\mathbf{x}_k$ and another point from previous iterations $\mathbf{x}_j$ is smaller than 10^{-10} in all dimensions of $\mathbf{x}$ and the objective function f_k is also equal to f_j with a difference of maximum 10^{10}, then execution is also terminated.

Note that these errors do not occur often, the program was able to successfully find the global optimum for most of the optimization problems tested without termination.

5. Initial Optimization

This section describes the initial optimization on the simplified problem with two variables. All other variables were set to constant values in the feasible domain.

5.1. Straight Design

Two variables: w_b and F were optimized to investigate the implementation of the SQP algorithm. The other variables, h_f, v_a and v_b were set to 1.0, 2.0 and 1.0 respectively such that these lie inside the feasible domain. The initial point was set to $[w_b F] = [1, 1]$ and the SQP algorithm was executed. The result is shown in Fig. 6. As can be seen, the algorithm converges along constraint g_{ca} towards the optimum of $[w_b F] = [2.2523.57]$ mm, N. The minimized value of the objective function is then 0.145 mm^2/N, thus the maximum strength equals 6.91 N/mm^2 for this configuration. Constraints g_{ca} and g_{tb} are active. It takes on average 4 seconds till the solution is found.
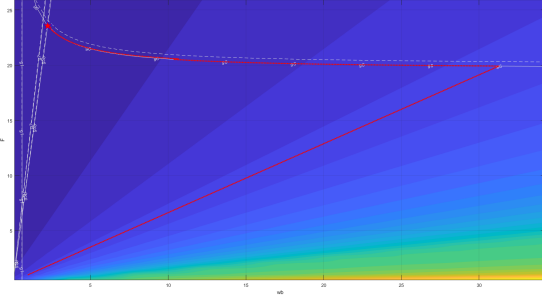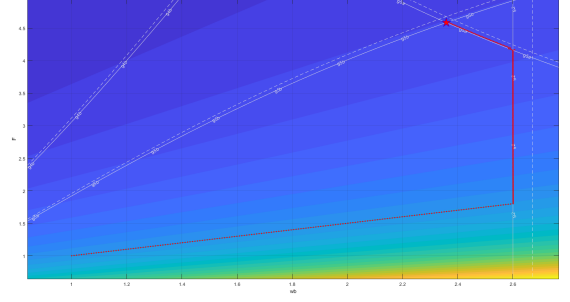

Fig. 6. The optimization steps taken by the SQP algorithm for the design variables w_b and F in the straight design. The dashed line shows the infeasible domain.

It is remarkable that the `quadprog` functions updates along the isolines of the objective instead of along the direction of the steepest descent towards the optimum. The cause might be that the objective is a non-convex function, which the `quadprog` function is not able to handle properly and then automatically moves along the isolines till encountering a constraint.

The KKT conditions were also checked. The feasibility conditions are satisfied because all inequality constraints are smaller than zero. Constraints g_{ca} and g_{tb} are treated as active, setting $\frac{\partial L}{\partial x} = 0$, gives two non-zero Lagrangian multipliers μ of 0.116 and 0.0217. Since $\mu > 0$, the KKT conditions are satisfied. Because not all constraint functions, neither the objective are convex, it cannot be concluded that this is the global optimum from the KKT conditions merely. However, when looking at contour plot, the found optimum seems to be the global optimum since it lies just in the feasible domain and minimizes the objective function.

5.2. Diagonal Design

The same SQP algorithm was also tested on the diagonal design. Again, w_b and F were optimized with an initial value of $[w_b F] = [1, 1]$. The other design variables w_a and L were set to 1.0 and 3.0 respectively. Fig. 7 shows the result, where w_b and F converge to 2.35 mm and 4.59 N respectively. This gives a minimized objective of 0.732 mm^2/N, equal to a maximum strength of 1.37 N/mm^2. Constraint g_{5a} and g_{5b} are then active and it takes 5 seconds on average till the optimum is found.

Fig. 7. The optimization steps taken by the SQP algorithm for the design variables w_b and F in the diagonal design. The dashed line shows the infeasible domain.

Looking at the KKT conditions, the optimum lies in the feasible domain since all inequality constraints are smaller than zero, and therefore satisfied. Treating constraints g_{5a} and g_{5b} as active gives two non-zero Lagrangian multipliers μ of 0.023 and 0.71. Since all multipliers are larger than or equal to zero, the KKT conditions are satisfied and the SQP algorithm has found a local optimum. Still, the constraints are not so it cannot be concluded that this is a global optimum from the KKT conditions only. Observing the contour plot, it can be seen that the objective function is minimized at the optimum found while all constraints are satisfied. Therefore, the SQP algorithm found a global optimum in this case as well.

Note that the maximum strength values for the straight vs diagonal design are not comparable yet, since the other design variables were set at an arbitrary value in the feasible domain.

6. Actual Optimization

6.1. Straight Design

6.1.1. Results

The full optimization problem was run with the same SQP implementation. After 7 seconds on average, the algorithm converged to an optimum of 0.1359 mm^2/N, equal to a maximum strength of 7.36 N/mm^2. The values for the variables are presented in Table 4. It can be observed that the own implemenation of the SQP algorithm converges towards a slightly lower optimum than fmincon while still satisfying all constraints, the maximum value of the constraint functions is -2.275 $\cdot 10^{-11}$.

Table 4: The result of the own implementation of the SQP algorithm vs the MATLAB SQP solver fmincon for the straight design.

Variable	SQP - Own implementation	SQP - fmincon
Objective	0.135903	0.137964
Active constraints	g_d g_{ta} g_{tb} g_{ca} g_{zb}	g_d g_{ta} g_{tb} g_{ca} g_{zb}
w_b	2.685701	2.685714
v_a	2.568289	2.668029
v_b	1.031711	0.931971
h_f	1.202763	1.086396
F	33.914224	30.636365

6.1.2. KKT Conditions

Then the KKT conditions were checked. The optimum lies in the feasible domain since all constraints are equal to or smaller than zero. Constraints g_d, g_{ta}, g_{tb}, g_{ca} and g_{zb}

12

Table 5: The sensitivities for the straight design case.

	$\frac{df}{dx}$	$\frac{dg_1}{dx}$	$\frac{dg_{2a}}{dx}$	$\frac{dg_{2b}}{dx}$	$\frac{dg_3}{dx}$
$\frac{dg}{dw_b}$	0.041	-1.667	0	0	0
$\frac{dg}{dv_a}$	0	0	-3.333	0	0
$\frac{dg}{dv_b}$	0	0	0	-3.333	0
$\frac{dg}{dh_f}$	0.097	0	0	0	-5
$\frac{dg}{dF}$	-0.004	0	0	0	0
	$\frac{dg_4}{dx}$	$\frac{dg_{5a}}{dx}$	$\frac{dg_{5b}}{dx}$	$\frac{dg_6}{dx}$	$\frac{dg_7}{dx}$
$\frac{dg}{dw_b}$	0	0	-0.372	0.064	-0.372
$\frac{dg}{dv_a}$	0.278	0	0	-0.389	0
$\frac{dg}{dv_b}$	0.278	0	0	0	-0.969
$\frac{dg}{dh_f}$	0	-0.832	-0.832	0	0
$\frac{dg}{dF}$	0	0.029	0.029	0.029	0.029

are active. The Lagrangian multipliers for constraints g_d, g_{tb}, g_{ca} and g_{zb} are 0.022, 0.0075, 0.11, 0.017 and 0.0069 respectively. All multipliers μ are larger than or equal to zero. Therefore the KKT conditions are satisfied and the design variables found are a local optimum. A global optimum is not guaranteed since not all objective and constraint functions are convex, however as the objective is lower than the MATLAB fmincon implemenation while still satisfying all constraints, it is assumed that the global optimum is found by our own implementation.

6.1.3. Sensitivity Analysis

Table 5 present the sensitivities of the objective function and constraints with respect to the design variables. It is remarkable that the magnitudes of the sensitivities varies a lot. This means that some constraints increase much when changing a certain design variable while another might only increase or decrease slightly for the same change. Note that these results match the monotonicity analysis considering the sign of the first order derivatives. The green cells evaluate the boundedness by the active constraints, one cannot decrease the objective function without increasing the objective function which is visible from the opposite sign of the two partial derivatives.

The logarithmic sensitivities of the objective function with respect to the design variables were also evaluated. These are 0.817, 0, 0, 0.857 and -1 for the design variables w_b, v_a, v_b, h_f and F respectively. It is not possible to relax the constraints that are active on F since these consists of stress limits rather than design choiches. Therefore, to lower the objective function if necessary, it is recommended to relax constraint g_d by increasing the upper limit for L.

6.2. Diagonal Design

6.2.1. Results

The diagonal design converges after around 6 seconds. It reaches an optimum value of 0.5008 mm^2/N, equal to a maximum strength of 1.996 N/mm^2. Table 6 shows the optimal values for the design variables. It is remarkable that the own implementation converges towards another optimum, which does not match the real optimum, variable L is slightly offset its true optimal value. This can be due to two reasons. The SQP implementation selects the active set based on the constraints that are violated in the current iteration, where

Variable	SQP - Own implementation	SQP - fmincon
Objective	0.500837	0.497616
Active constraints	g_{1a} g_{4a} g_{5a} g_{5b}	g_{1a} $g_{3,2}$ g_{5a} g_{5b}
w_a	0.3	0.3
w_b	0.667658	0.666732
L	3.270938	3.6
F	1.932080	1.942727

Table 6: The result of the own implementation of the SQP algorithm vs the MATLAB SQP solver fmincon for the diagonal design.

Table 7: The sensitivities for the diagonal design case.

	$\frac{df}{dx}$	$\frac{dg_{1a}}{dx}$	$\frac{dg_{1b}}{dx}$	$\frac{dg_2}{dx}$	$\frac{dg_{3,1}}{dx}$
$\frac{dg}{dw_a}$	0.518	-3.333	0	0.278	0
$\frac{dg}{dw_b}$	0.518	0	-3.333	0.278	0
$\frac{dg}{dL}$	0	0	0	0	-0.556
$\frac{dg}{dF}$	-0.259	0	0	0	0
	$\frac{dg_{3,2}}{dx}$	$\frac{dg_{4a}}{dx}$	$\frac{dg_{4b}}{dx}$	$\frac{dg_{5a}}{dx}$	$\frac{dg_{5b}}{dx}$
$\frac{dg}{dw_a}$	0	-5.633	0.65	-10.791	1.917
$\frac{dg}{dw_b}$	0	1.033	-1.233	2.076	-3.474
$\frac{dg}{dL}$	0.278	-0.306	-0.192	-0.032	-0.05
$\frac{dg}{dF}$	0	0.518	0.325	1.035	1.035

g_{4a} is selected incorrectly. The reason might be that g_{4a} is a non-convex function that the used `quadprog` function has difficulties with. After reaching $L = 3.27$ it is not able to escape from the non-convex feasible space boundary.

6.2.2. KKT Conditions

The findings of this result were verified with the KKT conditions. The feasibility conditions are satisfied since all constraints are smaller than or equal to zero. The Lagrangian multipliers were checked for the active constraints, which are 0.060, -0.039, 0.166 and 0.374 for constraints g_{1a}, g_{4a}, g_{5a} and g_{5b} respectively. Indeed, the Lagrangian multiplier for g_{4a}, that constrains the value of design variable L, is smaller than zero. Therefore, the KKT conditions are not satisfied and the point that was found is not an optimum.

When evaluating the Lagrangian multipliers obtained with fmincon, these are equal to 0.051, 0.0305, 0.129 and 0.369 for constraints g_{1a}, g_{4a}, g_{5a} and g_{5b} respectively. The magnitudes of the multipliers matches the magnitude of the multipliers found by our own implementation. This makes sense, because the magnitide of the Lagrangian multipliers shows how strongly changes in constraints affect the objective function. This relative importance of the constraint functions does of not differ between both implementations.

6.2.3. Sensitivity Analysis

Table 7 show the sensitivities for the diagonal design case, where these signs of the first order derivatives matches the monotonicity analysis. The green cells show the boundedness of the design variables, it is not possible to decrease the objective without increasing of the constraint functions.

The logarithmic sensitivities of the objective function are 0.31, 0.69, 0 and -1 for design variables w_a, w_b, L and F respectively. Constraint g_{4a}, g_{5a} and g_{5b} cannot be relaxed because these involve stress limitations rather than design choices. Therefore, it is recommended to relax constraint g_{1a} by decreasing $w_{a,\min}$ to lower the objective function,

which can be achieved by selecting another printer with a smaller nozzle diameter.

7. Conclusion

This paper aimed to determine the optimal design variables for a mechanically interlocking structure of two incompatible materials. Two designs were considered, a straight design and a diagonal design. After optimizing with a self-implemented SQP algorithm, it was found that the straight interlocking design outperforms the diagonal design. The maximum stress which can be reached with the straight design is around three times as high as the maximum stress which can be achieved using the diagonal setup. The design variables w_b, v_a, v_b, h_f and F are equal to 2.68, 2.56, 1.03, 1.20 and 33.91 respectively. The tensile strength of the interlocking structure is then 7.36 MPa. When comparing this ultimate tensile strength of the interlocking structure to the tensile strength of the weakest of the two materials, Ultimaker PolyPropylene of 10.5 MPa, the tensile strength reaches 70 % of the base material strength. This value is relatively high considering the weak chemical bonding between PP and most other thermoplastics.

7.1. Recommendations

To account for inaccuracies in the loading conditions, material properties and in manufacturing process, it is recommended to introduce safety factors on a design variables obtained which will slightly increase the obtained optimum. For the manufacturing, a deposition accuracy of 0.1 mm is a reasonable guesstimate for most desktop FDM 3D printing systems.

The optimum is found at the intersection of several constraint surfaces, each of which has a different gradient at the optimum. Adding the deposition accuracy to the optimum obtained gives a random perturbation in the design space, the expected stress at the optimum might be lower compared to a different reference point which is a bit further down along the least steep surface.

Looking at the graphs in Fig. 4 and the sensitivities it makes sense to choose a design with a slightly lower h_f and w_b than the optimum of the straight design. The sensitivity of $\mathbf{x}_i$ in one of the active constraints $\mathbf{g}_i$ can then be computed with:

$$\frac{\partial f}{\partial \mathbf{x}_i} + \sum^{j \neq i} \frac{\partial f}{\partial \mathbf{x}_j} \left(\frac{\partial \mathbf{g}_i}{\partial \mathbf{x}_j} \right)^{-1} \frac{\partial \mathbf{g}_i}{\partial \mathbf{x}_i}$$

In this way, one could compute the expected ultimate strength considering a random perturbation of the design. However, finding other optimal design parameters given manufacturing inaccuracies falls outside the scope of the current work.

Depending on the application of the interlocking structure, different constraint values might apply. For other materials the optimum is expected to shift towards another location. Though the sensitivities show the dependency of the objective function and constraints with respect to the design variables, deriving the dependency of the actual optimum with respect to the material parameters has not been investigated. Another important consideration are the values set for the design constraints. These were chosen based
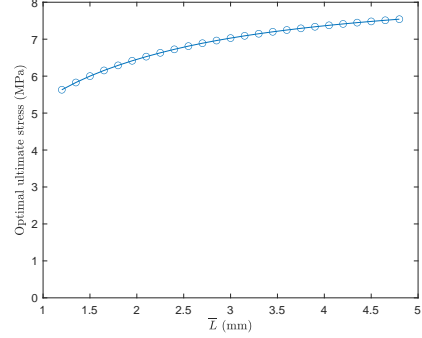
Fig. 8. The optimal strength for various values of the design constraint $L_{\max}$.

on particular printer limitations, however if these are modified to accomodate for other manufacturing resources the optimum point is expected to shift. For example, the constraint value $L_{\max}$ was varied. Figure 8 shows that using a bigger design space can achieve higher values for the objective function.

7.2. Limitations and Future work

In the current optimization problem, the active set and the lambda update strategy require more tuning in order to work for a wider range of design problems if not with better heuristics then with local iterations to get $\mathbf{x}$ and $\boldsymbol{\lambda}$ closer to their intended values. Moreover the `quadprog` encountered problems when updating the design variables for non-convex objective functions, which drove the unconstrained optimization along isolines rather than in the direction of the steepest descent.

Considering the optimization strategy, also different algorithms can be experienced with. For example, if the governing equations are not directly or differentiable, for example when the *max* out of two variables is taken as suggested, other algorithms like the genetic algorithm, Powell's Conjugate Directions method or Nelder and Mead Simplex method are recommended to be exploited.

Another limitation is that the manufacturing constraint that h_f should be an integer multiple of $h_{\min}$ was not ac-

counted for. SQP doesn't seem to be well suited for the problem at hand, however when looking at the sensitivities it is recommended to round this value up to relax the constraints.

The mathematical problem definition proposed has strong assumptions with respect to the homogeneity of stress distributions throughout the part, while in reality the disctribution of stress is expected to be heterogenous. Specifically the validity of the diagonal model is hard to verify, since the angles it hard to analyze the anisotropic behavior. Also factors such as friction can prove to be significant which has not been accounted for.

One line of future research is directed at different types of interlocking designs. Does high genus interlocking designs outperform 2D dovetail type interlocking designs for more flexible materials? How would the optimal interlocking design look for different forces, like shear, or a vertically applied force? These are to be investigated in future research.